




Article

Modeling of Nitrification Kinetics in a Respirometric Biosensor under Suboptimal Conditions

Andrzej Woznica ^{1,2}, Jerzy Karczewski ², Czesław Klis ³, Jacek Długosz ⁴, Przemysław Ziemiński ², Agnieszka Nowak ^{2,*} and Tytus Bernas ⁵

¹ Silesian Water Centre, University of Silesia in Katowice, 40-007 Katowice, Poland; andrzej.woznica@us.edu.pl

² Institute of Biology, Biotechnology and Environmental Protection, Faculty of Environmental Science, University of Silesia in Katowice, 40-032 Katowice, Poland; jerzy.karczewski@us.edu.pl (J.K.); przemyslaw.ziemski@us.edu.pl (P.Z.)

³ Private Researcher, 40-844 Katowice, Poland; cz.klis@gmail.com

⁴ Institute for Ecology of Industrial Area, 40-844 Katowice, Poland; dlugosz@ietu.katowice.pl

⁵ VCU Microscopy Core Facility at Virginia Commonwealth, University School of Medicine, Charlottesville, VA 23298, USA; tytus.bernas@vcuhealth.org

* Correspondence: agnieszka.a.nowak@us.edu.pl

Abstract: Sensitive detection with cell biosensors requires optimization of their working conditions and standardization of the response in variable physicochemical conditions. The introduction of an analyte to a sensor, which contributes to this variability, may account for the modeling of microbial metabolism. We constructed a multiparameter model of a water toxicity sensor of Automatic Biode-tector for Water Toxicity (ABTOW), developed by our group and based on nitrifying bacteria. The model describes the kinetics of nitrification as a function of four orthogonal parameters: temperature, pH, oxygen and ammonium concentration. Furthermore, we characterized the signal-to-noise ratio (SNR) of the ABTOW readout as a function of these parameters. Thus, a region of parameter space corresponding to optimal ABTOW operation is identified and its sensitivity quantified. We applied the model to describe the ABTOW performance in non-equilibrium conditions produced by rapid changes in pH and temperature. In sum, the model based on four physicochemical parameters describes changes in the biosensor's activity, the biological element of which are nitrifying bacteria characterized by simple chemolithoautotrophic metabolism. The description of reaction kinetics through multiparameter modeling in combination with stability analysis can find application in process control in biotechnology, biodetection and environmental research.

Keywords: ABTOW; nitrification kinetics; suboptimal conditions; modeling



Citation: Woznica, A.; Karczewski, J.; Klis, C.; Długosz, J.; Ziemiński, P.; Nowak, A.; Bernas, T. Modeling of Nitrification Kinetics in a Respirometric Biosensor under Suboptimal Conditions. *Water* **2022**, *14*, 2031. <https://doi.org/10.3390/w14132031>

Academic Editor: Quanfa Zhang

Received: 13 May 2022

Accepted: 22 June 2022

Published: 25 June 2022

Publisher's Note: MDPI stays neutral with regard to jurisdictional claims in published maps and institutional affiliations.



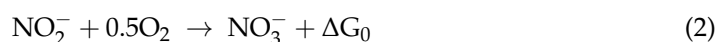
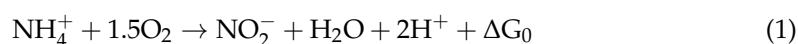
Copyright: © 2022 by the authors. Licensee MDPI, Basel, Switzerland. This article is an open access article distributed under the terms and conditions of the Creative Commons Attribution (CC BY) license (<https://creativecommons.org/licenses/by/4.0/>).

1. Introduction

Mitigation of the risk caused by contamination of drinking water requires sensitive and inexpensive detection methods compatible with continuous, long-term monitoring. The former can be achieved with traditional physicochemical analysis. However, the classic approach may not produce a real-time readout [1,2]. This problem can be solved with biosensors based on microbial cells. For instance, standard methods include colorimetric methods (e.g., cyanide detection); atomic absorption spectroscopy methods (e.g., heavy metals detection); or chromatographic methods (e.g., using High-Performance Liquid Chromatography (HPLC) or Gas Chromatography (GC) for polycyclic aromatic hydrocarbons (PAH) or insecticides detection, respectively) [3,4]. All of them require appropriate sample preparation, and the analysis of each of them takes at least several minutes. Thus, biosensors based on immobilized bacteria provide the opportunity for real-time water quality monitoring. The application of microbial cells in water biosensing is a rapidly growing field [5–8]. Bacteria may be easily immobilized without loss of metabolic activity, providing durable and inexpensive sensing elements. The advantage of nitrifying bacteria is the high

consumption of oxygen in their metabolism (especially during ammonium oxidation), with a simultaneous slight increase in biomass which results from the low energy efficiency of the nitrification processes. This allows for high metabolic stability of the microorganisms used as the biological element of the biosensor for a relatively long period of time [9–12].

The Automatic Biodetector of Water Toxicity (ABTOW), developed by our group, is an example of this approach. The dynamics of biofilm development, optimal working conditions and the response of ABTOW to different xenobiotics have been determined empirically [1,2,12,13]. The optimal state may be disturbed by the introduction of examined water to ABTOW, resulting in a false positive signal. Changes in physicochemical conditions (temperature, pH or oxygen concentration), caused by the introduction of the analyte, can be accounted for in a model of microbial metabolism. Owing to the diversity of metabolites and processes, only selected reactions (or relationships) are included and parameterized in models [14]. The standard approach includes the determination of stoichiometric and kinetic coefficients of each process separately [15–17]. Individual reactions are then combined to form a numerical model of a sensor. We adopted this approach for ABTOW, where nitrification is catalyzed by two groups of ubiquitous lithoautotrophic bacteria. The first group comprises ammonium-oxidizing bacteria (AOB), and the second, nitrite-oxidizing bacteria (NOB) [1,18]. We used stoichiometry proposed by Wiesmann et al. [19], which takes into account both the anabolism and catabolism of 1 mol NH_4^+ and NO_2^- :



This electron flow generates a proton gradient, which participates in adenosine triphosphate (ATP) synthesis [20]. When ammonium is the electron source, all the produced nitrite is consumed immediately in ABTOW [1]. Hence, we focused on the first stage of nitrification. We constructed a kinetic model of the ABTOW operation where oxygen consumption was characterized as a function of pH, temperature and concentrations of substrates.

The objective of this study was the optimization of the model for the search for optimal pH and temperature values for measurement precision: reading changes in oxygen concentration; shortening the retardation of the reaction time on the environmental changes (e.g., pollutants, toxic substances); and standardization of the model enabling the recognition of types of environmental changes in various ranges for different concentrations.

2. Materials and Methods

2.1. Immobilization, Growth and Activity Quantification of Bacteria in ABTOW

Consortia of nitrifying bacteria were isolated from activated sludge from the wastewater treatment plant Klimzowiec, Katowice (Upper Silesia, Poland). Initially, the bacteria were isolated after the activated sludge inoculation to the selection media specific for nitrifiers according to the protocol described by Mac Donald and Spokes [21]. The consortium of nitrifiers was characterized previously using genetic and biochemical methods [1,12]. Next, consortia of nitrifying bacteria were grown in an 8 L laboratory-scale reactor as a fed-batch culture in physicochemical conditions described previously. The biomass from this bioreactor was then immobilized in polyurethane sponges (length 100 mm, diameter 25 mm) located horizontally in polystyrene tubes (120 mm long, diameter 25 mm) in a flow system in ABTOW [1]. The layout of ABTOW, its calibration and its operation, were described by Woznica et al. [1,2,12,13]. Briefly, the bacterial biofilms were grown in bioreactors for a minimum of 14 days to obtain their stable structure and physiology. A mineral medium with ammonium (3.4 mM) as an electron donor and oxygen (0.24 mM) as an electron acceptor was used. The medium with tap water, pumped at a rate of 100 mL min^{-1} , was maintained at 295 K (22 °C) and pH of 7.5 [1]. Oxygen consumption rate (v) of AOB was measured as a difference between the outlet and inlet oxygen concentration corrected for flow retardation. The correction of the signal from the electrodes consisted in averaging the measurements from four electrodes localized between the inlet and outlet of each of three

sequentially connected reactors. In the experiment where the influence of temperature on the activity of nitrifying bacteria was investigated, the medium and water were initially incubated in an ice bath (278 K) and then gradually heated to higher temperatures (up to 318 K). The pH of the medium was regulated with sodium hydroxide and sulfuric acid. The measurements were recorded in 5 s intervals, and the ABTOW activity was represented as a function of time ($v(t)$) using quasi-Newton estimation [1,2,12,13].

2.2. Statistical Analysis

Coefficients of the kinetic equations were estimated using nonlinear curve fitting, implemented in OriginPro 9.1 (OriginLab Corporation) or Statistica 13 (TIBCO software). The quality of the fit of theoretical and measurement data was evaluated using Pearson's chi-squared test (χ^2) and r^2 statistics.

The signal-to-noise ratio (SNR) was estimated as v/σ , where v is the expected (measured) value of oxygen consumption rate, and σ is a measure of fluctuations resulting from the stochastic nature of the processes [8]. The signal-to-noise ratio (SNR) is estimated as v/σ , where v is the expected (measured) value of oxygen consumption rate as σ is a measure of fluctuations resulting from the stochastic nature of the processes [22].

3. Results

3.1. Construction of the ABTOW Model

The performance of a microbial biosensor, including ABTOW is determined by fixed parameters: biosensor architecture (the 3D spatial organization of immobilized bacterial colonies in polyurethane sponge) and the density of bacteria and their distribution [1,2,12,23]. Substrate concentration, pH and temperature may vary during biosensor operation (Figure 1A,B).

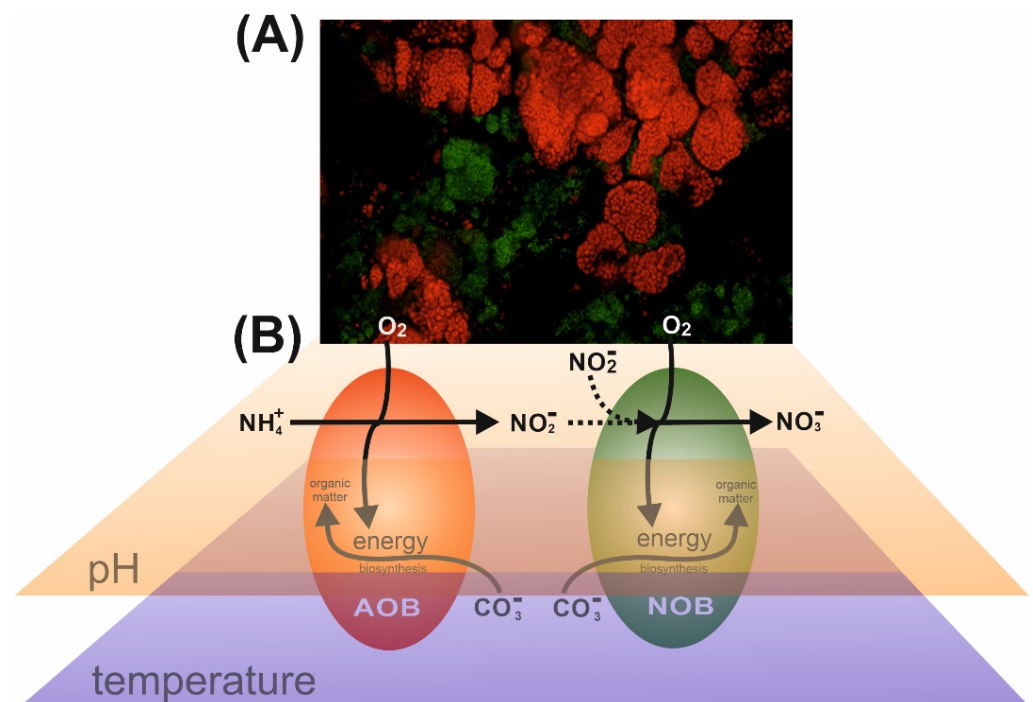


Figure 1. Biosensor based on consortia of nitrifying bacteria (ABTOW). (A) spatial arrangement of colonies of ammonium-oxidizing bacteria (AOB, red) and nitrite-oxidizing bacteria (NOB, green) in an ABTOW. (B) Schematic view of nitrification, catalyzed by AOB (first stage of nitrification) and NOB (second stage).

We analyzed the influence of these variables on AOB activity. Ammonium oxidation was assumed to follow Michaelis–Menten kinetics for a two-substrate reaction (Equation (3)) in the absence of products [1,12]:

$$v_{\text{-AO}}(c_A, c_O) = \frac{c_E}{\frac{1}{k_E} + \frac{1}{k_A c_A} + \frac{1}{k_O c_O} + \frac{1}{k_{\text{AO}} c_O c_A}} \quad (3)$$

where: c_A , c_O , c_E are concentrations of ammonium (mM), oxygen (mM) and the enzyme (ammonium oxidase), respectively; k_A , k_O and k_{AO} are second and third-order rate constants and k_E is the apparent first-order rate constant (saturated enzyme).

The equation can be rearranged to:

$$v_{\text{-AO}}(c_A, c_O) = \frac{k_E c_E c_A c_O}{\frac{k_E}{k_{\text{AO}}} + \frac{k_E}{k_A} c_O + \frac{k_E}{k_O} c_A + c_O c_A} \quad (4)$$

Substituting single-substrate Michaelis–Menten constants $K_A = k_E/k_A$ and $K_O = k_E/k_O$ and the maximum rate of the two-substrate reaction ($V_{\text{max}} = k_E c_E$), one obtains:

$$v_{\text{-AO}}(c_A, c_O) = \frac{V_{\text{max}} c_A c_O}{\frac{k_E}{k_{\text{AO}}} + K_A c_O + K_O c_A + c_O c_A} \quad (5)$$

Approximating k_E/k_{AO} with a product of K_A and K_O , one may represent the rate of the two-substrate reaction as a product of two single-substrate Michaelis–Menten equations:

$$v_{\text{-AO}}(c_A, c_O) = \frac{V_A c_A}{K_A + c_A} * \frac{V_O c_O}{K_O + c_O} = v_A(c_A) * v_O(c_O) \quad (6)$$

The maximum velocities (V_A and V_O) correspond to the situation where the other substrate (ammonium (mM) and oxygen (mM), respectively) is present in excess and thus does not limit the rate of the reaction. Hence, the measured values of K_O and K_A are independent of the other substrate. It is assumed that temperature (K) and pH influence V_{max} but not the reaction constants of the substrates with ammonium oxidase. Thus, the parameters (pH, temperature, ammonium and oxygen concentration) are regarded as orthogonal, and their influence may be expressed using rate functions (v), with the maxima normalized to unity. Accordingly, with V_{max} measured in optimal temperature and pH, one obtains a combined model of the reaction:

$$v(c_A, c_O, \text{pH}, T) = V_{\text{max}} * v_A(c_A) * v_O(c_O) * v_{\text{pH}}(\text{pH}) * v_T(T) \quad (7)$$

Correction for the temperature dependence of oxygen solubility in water was introduced to ensure exact parameter orthogonality. Moreover, as kinetic studies were conducted in the stationary phase of the biofilm growth, the biomass of bacteria is assumed to undergo negligible changes during ABTOW operation [1,2].

3.2. Dependence of Nitrification Rate on the Substrate Concentration

Initial oxygen consumption rate (v) was measured at varying concentrations of 0 to 4 mM of ammonium as an electron donor (Figure 2A). One should note that v was estimated by extrapolation to a time of 0 when nitrite was absent. Moreover, in ABTOW, nitrite concentration was negligible when ammonium was added as an electron source [2]. Thus, the observed changes of v corresponded to AOB activity. The respective parameters are: $63.87 \pm 0.92 \mu\text{mol} \cdot \text{min}^{-1}$ (V_A) and $0.045 \pm 0.004 \text{ mM}$ (K_A). Small parameter fit errors and a large correlation coefficient ($r^2 = 0.99$) indicate that the Michaelis–Menten model was sufficient to describe the observed kinetics (Figure 2A).

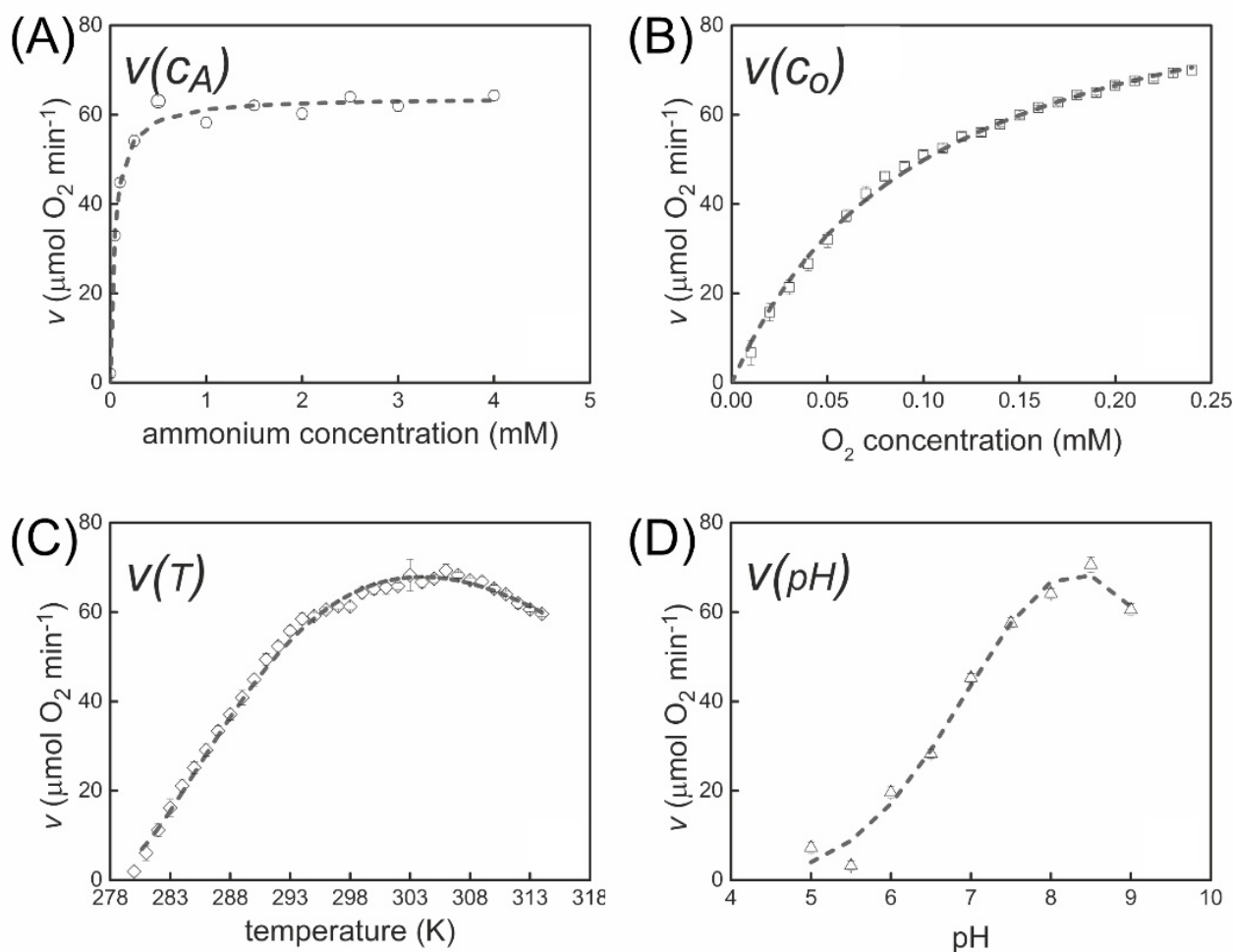


Figure 2. Rate of ammonium oxidation by AOB. Dependence of the rate on: (A) ammonium $v(c_A)$. (B) Oxygen $v(c_O)$ concentration (Michaelis–Menten models). (C) Temperature $v(T)$ modelled with Schoolfield and (D) pH $v(\text{pH})$ modelled with the GausAmp equation. Experimental data are marked with symbols (error bars SD), and fitted model curves are marked with dotted lines.

Similarly, the rate was measured at varying initial concentrations of electron acceptor (O_2). It can be assumed that the nitrite produced by AOB is immediately consumed by NOB and the ammonium oxidation corresponded to 75% of the total oxygen consumption in ABTOW [1,2]. The consumption rate ($v(c_O)$) was expressed as a function of oxygen concentration (Figure 2B) using a standard Michaelis–Menten equation:

$$v_O(c_O) = V_O \cdot \frac{c_O}{K_O + c_O} \quad (8)$$

where: V_O ($\mu\text{mol} \cdot \text{min}^{-1}$) is the maximum rate, c_O (mM) is oxygen concentration and K_O (mM) is the Michaelis–Menten constant.

The equation parameters, determined by using nonlinear curve fitting are 88.41 ± 1.37 (V_O) and 0.100 ± 0.001 (K_O). The model described well the observed kinetics (Figure 2B), as indicated by a large correlation coefficient ($r^2 = 0.99$). However, the range of measurements was limited by the performed solubility of oxygen in a nutrient medium (0.24 mM at 295 K). Thus, the rate plateau (predicted by the model) could not be reached. Therefore, other measurements (pH, temperature and ammonium concentration) were performed at $v(c_O)$, corresponding to $62.41 \mu\text{mol min}^{-1}$.

3.3. Temperature Dependence of Ammonium Oxidation

To determine dependence of the activity on temperature, the reactor was thermally isolated. The nutrient medium was cooled to 278 K (5 °C) and placed in a water bath at 318 K (45 °C). Thus, the rate (v_T) was measured in the temperature range from 278–318 K and described using the Arrhenius model, modified by Schoolfield [24]:

$$v_T(T) = V_T \cdot \frac{\frac{T}{T_o} \cdot \exp\left[\frac{E_a}{R} \cdot \left[\frac{1}{T_o} - \frac{1}{T}\right]\right]}{1 + \exp\left[\frac{E_l}{R} \cdot \left[\frac{1}{T_l} - \frac{1}{T}\right]\right] + \exp\left[\frac{E_h}{R} \cdot \left[\frac{1}{T_h} - \frac{1}{T}\right]\right]} \quad (9)$$

where: R ($\text{kJ}\cdot\text{K}^{-1}\cdot\text{mol}^{-1}$) is gas constant; E_a ($\text{kJ}\cdot\text{mol}^{-1}$) is the activation energy of nitrification; T_o (K) is the optimal temperature of the process; E_l ($\text{kJ}\cdot\text{mol}^{-1}$) is the activation energy of low-temperature enzyme denaturation, T_l (K) temperature of low-temperature denaturation; and E_h ($\text{kJ}\cdot\text{mol}^{-1}$) is the activation energy of high-temperature enzyme denaturation, T_h (K) temperature of high-temperature denaturation.

The model combined three components: increase in the reaction rate with temperature (numerator) and high- and low-temperature inactivation (denominator). The parameter values used to calibrate the model, in the units we used, are given in Table 1.

Table 1. Parameters of the ABTOW model.

Equation Parameter	Symbol	Value	Unit
maximum oxygen consumption rate	V_{\max}	70.62 ± 6.9	$\mu\text{mol}\cdot\text{min}^{-1}$
O ₂ Michaelis constant	K_O	0.1	mM
NH ₄ ⁺ Michaelis constant	K_A	0.04	mM
optimal pH	pH_{opt}	8.15 ± 0.05	-
difference between high pH and low pH when v is equal to $0.5 V_{\text{pH}}$	U	1.9 ± 0.09	-
the activation energy of AOB nitrification process	E_a	183 ± 23	$\text{kJ}\cdot\text{mol}^{-1}$
the activation energy of low-temperature enzyme denaturation	E_l	177 ± 22	$\text{kJ}\cdot\text{mol}^{-1}$
the activation energy of high-temperature enzyme denaturation	E_h	378 ± 21	$\text{kJ}\cdot\text{mol}^{-1}$
the optimal temperature of the process	T_o	298	K
the temperature of low-temperature denaturation	T_l	287 ± 0.7	K
the temperature of high-temperature denaturation	T_h	307 ± 12	K

The model adequately described the experimental data (Figure 2C). It may be noted the enzyme retains activity within an interval of 14 K (difference between $T_l = 286$ K and $T_h = 300$ K), while the optimal temperature (T_o) corresponds to 298 K (25 °C).

3.4. Effect of pH on the Ammonium Oxidation

The rate (v) was measured in the pH range from 5.0 to 9.5. In order to describe the pH dependence, several phenomenological models have been tested, including used polynomial models proposed for other enzymatic reactions. An adequate fit was provided by a modified Gaussian peak shape function (GaussAmp from Origin 9.1):

$$v_{\text{pH}}(\text{pH}) = V_{\text{pH}} \cdot \exp\left\{\frac{(-\ln(4) \cdot (\text{pH} - \text{pH}_{\text{opt}})^2)}{U^2}\right\} \quad (10)$$

where: V_{pH} is the rate at optimum pH (pH_{opt}), and U is the difference between high pH and low pH when v is equal to $0.5 V_{\text{pH}}$. The parameter values used to calibrate the model, in the units we used, are given in Table 1.

The model described well the experimental data (Figure 2D), as indicated by $r^2 = 0.98$. The optimal pH (pH_{opt}) was 8.15 ± 0.09 , which is higher than the standard value (see Section 2). The width of the pH interval where activity was greater than $0.5 V_{pH}$ is equal to 3.29 units. This value (U) indicates that the system is moderately sensitive to pH changes.

3.5. Dependence of ABTOW Sensitivity on the Stability of Measurement Conditions

It should be noted that, while the detected signal in the biodetector is proportional to the oxygen consumption rate, the detection uncertainty (error) is determined by the stability of the parameters (ammonium and oxygen concentration, pH and temperature):

$$\sigma_v^2 = \sigma_{C_a}^2 + \sigma_{C_o}^2 + \sigma_{pH}^2 + \sigma_T^2 + \sigma_n^2 \tag{11}$$

$$\sigma_p^2 = \frac{\partial v}{\partial p} \Delta p, p \in \{Ca, Co, pH, T\}, \sigma_n^2 = \text{const.} \tag{12}$$

where: σ_v^2 is the total variance of the oxygen consumption rate (v , Equation (7)), $\sigma_{\{Ca,Co,pH,T\}}^2$ are variances due to the instability of parameters (p) and σ_n^2 is the variance corresponding to the detector noise (Equation (11)).

The sensitivity of the biodetector (dynamic range) may be expressed as the signal-to-noise ratio (SNR):

$$\text{SNR} = \frac{v}{\sqrt{\sigma_v^2}} \tag{13}$$

The SNR increases with concentrations of ammonium and oxygen (Figure 3C,D). Conversely, only small changes are observed when the concentrations are significantly higher than their respective Michaelis–Menten constants (Figure 3C–E). Thus, SNR reaches a plateau above 1.5 mM concentration of ammonium (Figure 3C–E). On the other hand, SNR is limited by oxygen solubility (0.24 mM) since the plateau is not reached at this concentration. Therefore, the optimal performance for these two factors cannot be determined (Figure 3E). Not surprisingly, maximum SNR with respect to temperature and pH is reached within the range where these parameters provide a maximum oxidation rate (Figure 3F). This is due to the fact that the variances σ_p (calculated as derivatives) are equal to zero, and the total noise is only equal to σ_n (Equation (12)). However, as the rate deviates from V_{max} , fluctuations in temperature and pH produce increasing instability of rate measurement (compare green and blue curves in Figure 3A,B).

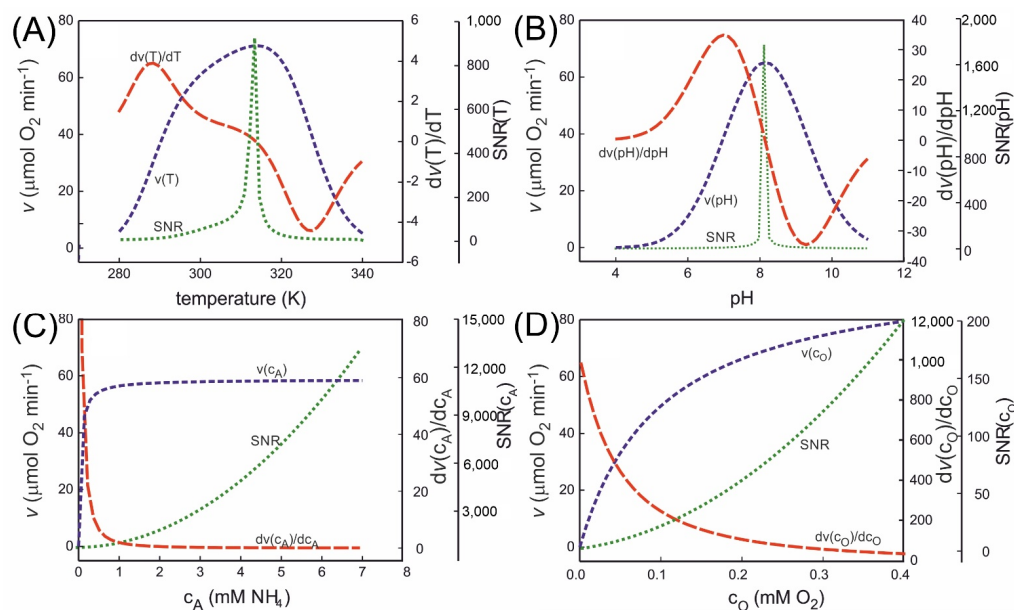


Figure 3. Cont.

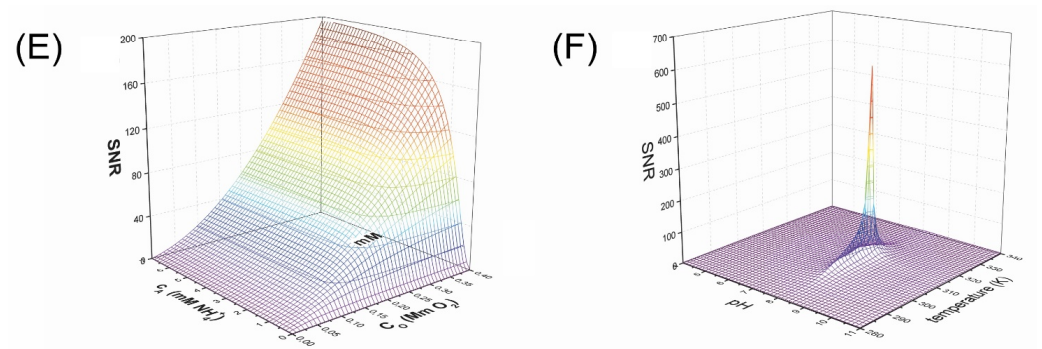


Figure 3. Dependence of signal-to-noise ratio (SNR) of ABTOW on the detection parameters: temperature (A), pH (B), concentrations of ammonium (C) and oxygen (D). The SNR is shown using dotted lines (green). The corresponding rates of nitrification are shown with a short dashed line (blue), while their derivative with a short dashed line (blue). Dependence of the SNR in the combined ABTOW model on substrate concentrations (E) and pH and temperature (F). The ranges of substrate concentration, temperature and pH, and units are analogous in all plots.

3.6. Performance of the Combined Model in Non-Equilibrium Conditions

The partial equations described in the previous paragraphs (Equations (8)–(10)) were combined into a single model of the biodetector (Equation (14), see also Equation (7)):

$$v = A_f \cdot V_{max} \cdot \left\{ \frac{c_A}{K_A + c_A} \cdot \frac{c_O}{K_O + c_O} \cdot \frac{(\ln(4) \cdot \exp[-(\text{pH} - \text{pH}_{opt})^2])}{U^2} \cdot \frac{\frac{T}{T_o} \cdot \exp\left[\frac{E_a}{R} \cdot \left[\frac{1}{T_o} - \frac{1}{T}\right]\right]}{1 + \exp\left[\frac{E_l}{R} \cdot \left[\frac{1}{T_l} - \frac{1}{T}\right]\right] + \exp\left[\frac{E_h}{R} \cdot \left[\frac{1}{T_h} - \frac{1}{T}\right]\right]} \right\} \quad (14)$$

The combined ABTOW model may be applied to account for changes in physicochemical parameters during the continuous operation of the biosensor. In order to verify this notion, the effects of varying temperature (Figure 4A) and pH (Figure 4B) were studied. The model described the oxygen consumption rate adequately in the present temperature increase from 281.55 K to 313.25 K. The rate increased initially with temperature to reach a plateau; then, above the optimum (108 K), a decrease was observed. The maximum rate of the temperature increase was 0.48 K per minute, which permitted the thermal equilibration of the sensor during the experiment.

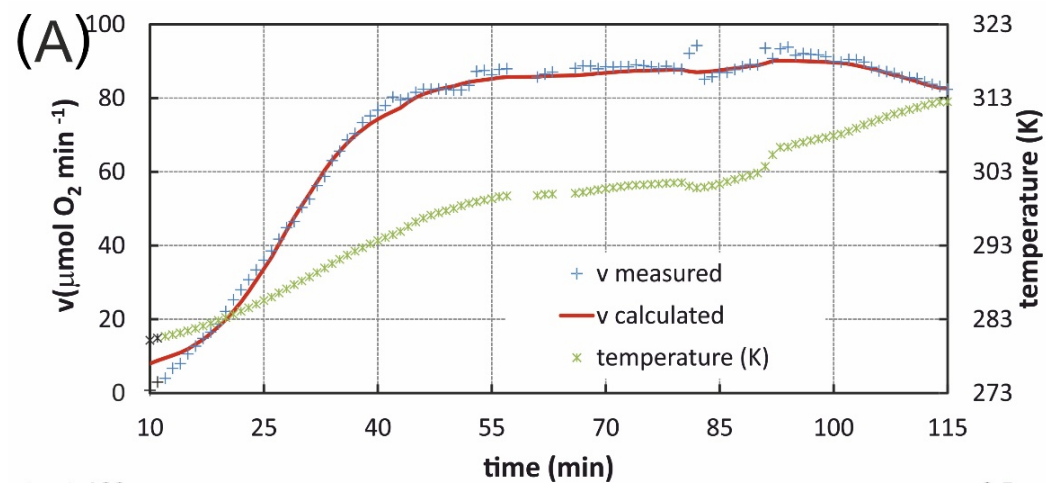


Figure 4. Cont.

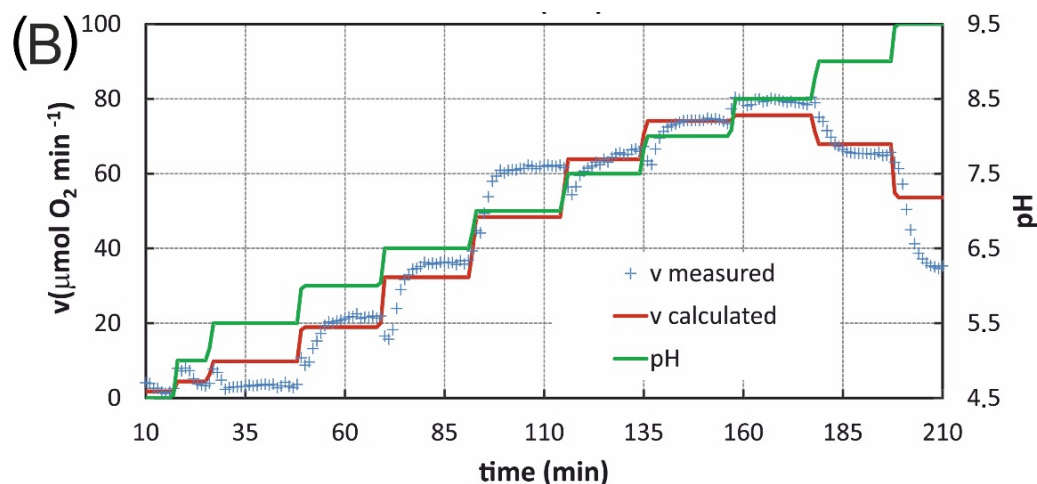


Figure 4. Performance of the ABTOW model in non-equilibrium conditions. Effects of temperature increase (A) and stepwise pH changes (B). Oxygen consumption (left Y-axis) and parameters (right Y-axis) are plotted against time (X-axis). Model prediction (red line) and experimental data (blue symbols) are plotted together with temperature (A, light green symbols) or pH (B, green line).

Likewise, the model correctly described the response of ABTOW to stepwise changes in pH (3–9.5) (Figure 4B). It may be noted that following pH change, oxygen consumption rate ABTOW reached a stable level after approximately 1.5 min. Therefore, it may be postulated that pH buffering contributes to the inertia of ABTOW, limiting its response velocity. All estimated parameters of the ABTOW model are summarized in Table 1.

4. Discussion

Reproducible on-line analysis of water quality requires standardization of the sensor output. Two approaches may be used to realize this goal in a biosensor based on live bacterial cells. First, the water entering the sensor may be pre-processed to maintain constant measurement conditions, for example: pH, temperature and concentration of reactants. Second, mathematical models can be used in post-processing to correct for the changes induced by the introduction of the analyte [25,26]. One can combine these two strategies to reduce the cost of operation and ensure the robust operation of a sensor. In particular, a model may drive the optimization of conditions at the pre-processing stage. Model performance depends on the proper selection of the parameters, which should be independent (orthogonal) and have a clear biological interpretation. The model complexity should be minimal to ensure its robust performance, which needs to be ascertained in a quantitative manner. The ABTOW model described here meets these requirements, making it possible to account for changes in physicochemical parameters of water in real-time during biosensor operation. Two approaches may be used to meet this goal in a biosensor based on live bacterial cells. First, water entering the sensor may be pre-processed to maintain constant measurement conditions: pH, temperature and concentration of reactants. Second, the results may be post-processed using appropriate mathematical models [25,26]. One can combine pre- and post-processing to increase the reliability of biosensors, reduce the cost of operation and quantify their detection limits. These factors are of particular importance in the detection of contaminants, where interpretation of the results is often automated. Moreover, pre-processing (optimization of conditions) is facilitated if the response of a biosensor can be predicted precisely. This task depends on the proper selection of the model parameters, which should be independent (orthogonal) and have a clear biological interpretation. The model complexity should be minimal to ensure robust performance, which needs to be ascertained in a quantitative manner. The ABTOW model presented here meets these requirements, thus making it possible to account for changes in physicochemical parameters of water during biosensor operation. Therefore,

it may be used to correct these changes in real-time and quantify the response caused by toxins.

The presented approach may be easily adapted to other microbial sensing systems. Similar models, which included the concentration of two substrates as parameters, have been described before [27,28]. However, an approximation of two-substrate reaction kinetics with a product of single-substrate Michaelis–Menten equations was provided without any justification in these papers. Here, we describe a two-substrate model for a single class of nitrifying bacteria [1,2] that may be adapted for other microbial species. Simultaneously, it should be noted that the model calibration (a set of parameters shown in Table 1 allowing for calculating the oxygen concentration) may be different for other bacteria. The parameter list may be expanded (e.g., ionic strength), and a combination of several models of this class may provide a general framework for the description of heterogeneous microbial communities. This bottom-up approach to complex systems may be applicable in modeling aquatic ecosystems, where simplifications are used to describe bacterial metabolism. Supplementing Estuary and Lake Computer Model (ELCOM) and Computational Aquatic Ecosystem Dynamics Model (CAEDYM) with modeling changes in biomass provides an example of this approach. Moreover, the characterization of stability and dynamic range of the output of the component models may improve the robustness of the composite ecosystem models. Quantification of sensitivity (SNR) is a simple and flexible way to approach this task.

To conclude, the presented modeling allows tracking the relationship between four parameters simultaneously. These parameters (concentration of oxygen and ammonium ions, temperature and pH) are crucial for the nitrification process. As a consequence, it enables the correction of biosensing determinations under changing initial conditions. Multiparameter modeling, combined with stability analysis, provides a simple, flexible and robust description of bioreaction kinetics and can be used for process control. This approach may be used in biotechnology, biosensing and environmental studies.

Author Contributions: Conceptualization, A.W., J.K. and C.K.; methodology, A.W. and P.Z.; software, J.K. and J.D.; validation, P.Z., J.K. and A.W.; formal analysis, A.W., T.B. and J.K.; investigation, A.W., J.K. and T.B.; resources, A.W. and A.N.; data curation, A.W. and J.K.; writing—original draft preparation, A.W.; writing—review and editing, A.N. and T.B.; visualization, A.W.; supervision, A.W.; project administration, A.W. and T.B.; funding acquisition, A.W. All authors have read and agreed to the published version of the manuscript.

Funding: This research was funded by the UE Innovate Economy Operational Programme, Priority 1 “Research and development of modern technologies”, Subaction 1.1.2 “An integrated system supporting the management and protection of the water reservoir”, grant number POIG 01.01.02-24-078/09.

Institutional Review Board Statement: Not applicable.

Informed Consent Statement: Not applicable.

Data Availability Statement: Not applicable.

Acknowledgments: We would like to thank the native speaker Frances While for the linguistic proofreading.

Conflicts of Interest: The authors declare no conflict of interest.

References

1. Woznica, A.; Nowak, A.; Beimfroh, C.; Karczewski, J.; Bernas, T. Monitoring Structure and Activity of Nitrifying Bacterial Biofilm in an Automatic Biodetector of Water Toxicity. *Chemosphere* **2010**, *78*, 1121–1128. [[CrossRef](#)] [[PubMed](#)]
2. Woznica, A.; Nowak, A.; Karczewski, J.; Klis, C.; Bernas, T. Automatic Biodetector of Water Toxicity (ABTOW) as a Tool for Examination of Phenol and Cyanide Contaminated Water. *Chemosphere* **2010**, *81*, 767–772. [[CrossRef](#)] [[PubMed](#)]
3. APHA (Ed.) *Standard Methods for the Examination of Water and Wastewater*; WPCF: Washington, DC, USA, 1995.
4. Herschy, R.W. Water Quality for Drinking: WHO Guidelines. In *Encyclopedia of Lakes and Reservoirs*; World Health Organization: Geneva, Switzerland, 2012; pp. 876–883. [[CrossRef](#)]
5. Eltzov, E.; Slobodnik, V.; Ionescu, R.E.; Marks, R.S. On-Line Biosensor for the Detection of Putative Toxicity in Water Contaminants. *Talanta* **2015**, *132*, 583–590. [[CrossRef](#)] [[PubMed](#)]

6. Gosset, A.; Ferro, Y.; Durrieu, C. Methods for Evaluating the Pollution Impact of Urban Wet Weather Discharges on Biocenosis: A Review. *Water Res.* **2016**, *89*, 330–354. [[CrossRef](#)]
7. Ejeian, F.; Etedali, P.; Mansouri-Tehrani, H.A.; Soozanipour, A.; Low, Z.X.; Asadnia, M.; Taheri-Kafrani, A.; Razmjou, A. Biosensors for Wastewater Monitoring: A Review. *Biosens. Bioelectron.* **2018**, *118*, 66–79. [[CrossRef](#)] [[PubMed](#)]
8. Hossain, S.M.Z.; Mansour, N. Biosensors for On-Line Water Quality Monitoring—a review. *Arab J. Basic Appl. Sci.* **2019**, *26*, 502–518. [[CrossRef](#)]
9. Nichols, D.; Ferguson, S. *Bioenergetics*, 4th ed.; Elsevier: Amsterdam, The Netherlands, 2013; ISBN 9780123884251.
10. Spieck, E.; Aamand, J.; Bartosch, S.; Bock, E. Immunocytochemical Detection and Location of the Membrane-Bound Nitrite Oxidoreductase in Cells of Nitrobacter and Nitrospira. *FEMS Microbiol. Lett.* **1996**, *139*, 71–76. [[CrossRef](#)]
11. Spieck, E.; Ehrich, S.; Aamand, J.; Bock, E. Isolation and Immunocytochemical Location of the Nitrite-Oxidizing System in Nitrospira Moscoviensis. *Arch. Microbiol.* **1998**, *169*, 225–230. [[CrossRef](#)]
12. Woznica, A.; Nowak, A.; Ziemski, P.; Kwasniewski, M.; Bernas, T. Stimulatory Effect of Xenobiotics on Oxidative Electron Transport of Chemolithotrophic Nitrifying Bacteria Used as Biosensing Element. *PLoS ONE* **2013**, *8*, e53484. [[CrossRef](#)]
13. Woznica, A.; Karcz, J.; Nowak, A.; Gmur, A.; Bernas, T. Spatial Architecture of Nitrifying Bacteria Biofilm Immobilized on Polyurethane Foam in an Automatic Biodetector for Water Toxicity. *Microsc. Microanal.* **2010**, *16*, 550–560. [[CrossRef](#)]
14. Kantartzi, S.G.; Vaiopoulou, E.; Kapagiannidis, A.; Aivasidis, A. Kinetic Characterization of Nitrifying Pure Cultures in Chemostate. *Glob. NEST J.* **2006**, *8*, 43–51.
15. Carrera, J.; Jubany, I.; Carvallo, L.; Chamy, R.; Lafuente, J. Kinetic Models for Nitrification Inhibition by Ammonium and Nitrite in a Suspended and an Immobilized Biomass Systems. *Process Biochem.* **2004**, *39*, 1159–1165. [[CrossRef](#)]
16. Jubany, I.; Carrera, J.; Lafuente, J.; Baeza, J.A. Start-up of a Nitrification System with Automatic Control to Treat Highly Concentrated Ammonium Wastewater: Experimental Results and Modeling. *Chem. Eng. J.* **2008**, *144*, 407–419. [[CrossRef](#)]
17. Jubany, I.; Lafuente, J.; Baeza, J.A.; Carrera, J. Total and Stable Washout of Nitrite Oxidizing Bacteria from a Nitrifying Continuous Activated Sludge System Using Automatic Control Based on Oxygen Uptake Rate Measurements. *Water Res.* **2009**, *43*, 2761–2772. [[CrossRef](#)]
18. Mota, C.; Head, M.A.; Ridenoure, J.A.; Cheng, J.J.; De Los Reyes, F.L. Effects of Aeration Cycles on Nitrifying Bacterial Populations and Nitrogen Removal in Intermittently Aerated Reactors. *Appl. Environ. Microbiol.* **2005**, *71*, 8565–8572. [[CrossRef](#)]
19. Wiesmann, U.; Choi, I.S.; Dombrowski, E.M. *Nutrient Removal in Fundamentals of Biological Wastewater Treatment Biological*; WILEY-VCH: Weinheim, Germany, 2007.
20. Gerardi, M.H. *Nitrification and Denitrification in the Activated Sludge Process*; (Google EBook); 2003; ISBN 0471461318. Available online: <https://books.google.vg/books?id=ccIKuXYNIBMC&printsec=frontcover#v=onepage&q&f=false> (accessed on 12 May 2022).
21. Macdonald, R.M.; Spokes, J.R. A Selective and Diagnostic Medium for Ammonia Oxidising Bacteria. *FEMS Microbiol. Lett.* **1980**, *8*, 143–145. [[CrossRef](#)]
22. Jokić, I.; Djurić, Z.; Radulović, K.; Frantlović, M.; Milovanović, G.V.; Krstajić, P.M. Stochastic Time Response and Ultimate Noise Performance of Adsorption-based Microfluidic Biosensors. *Biosensors* **2021**, *11*, 194. [[CrossRef](#)]
23. Karcz, J.; Bernas, T.; Nowak, A.; Talik, E.; Woznica, A. Application of Lyophilization to Prepare the Nitrifying Bacterial Biofilm for Imaging with Scanning Electron Microscopy. *Scanning* **2012**, *34*, 26–36. [[CrossRef](#)]
24. Zwietering, M.H.; de Koos, J.T.; Hasenack, B.E.; de Witt, J.C.; van't Riet, K. Modeling of Bacterial Growth as a Function of Temperature. *Appl. Environ. Microbiol.* **1991**, *57*, 1094–1101. [[CrossRef](#)]
25. Rinken, T.; Rinken, A.; Tenno, T.; Järv, J. Calibration of Glucose Biosensors by Using Pre-Steady State Kinetic Data. *Biosens. Bioelectron.* **1998**, *13*, 801–807. [[CrossRef](#)]
26. Van Hulle, S.W.; Volcke, E.I.; Teruel, J.L.; Donckels, B.; van Loosdrecht, M.C.; Vanrolleghem, P. Influence of Temperature and PH on the Kinetics of the Sharon Nitritation Process. *J. Chem. Technol. Biotechnol.* **2007**, *82*, 471–480. [[CrossRef](#)]
27. Davidson, E.A.; Samanta, S.; Caramori, S.S.; Savage, K. The Dual Arrhenius and Michaelis-Menten Kinetics Model for Decomposition of Soil Organic Matter at Hourly to Seasonal Time Scales. *Glob. Chang. Biol.* **2012**, *18*, 371–384. [[CrossRef](#)]
28. Rosso, L.; Lobry, J.R.; Bajard, S.; Flandrois, J.P. Convenient Model to Describe the Combined Effects of Temperature and pH on Microbial Growth. *Appl. Environ. Microbiol.* **1995**, *61*, 610–616. [[CrossRef](#)] [[PubMed](#)]